Supplementary Materials: Modulating Interfacial Charge Transfer Behavior through the Construction of a Hetero-Interface for Efficient Photoelectrochemical Water Splitting

Li Xu [1,†], Jingjing Quan [1,†], Li Xu [2,†], Meihua Li [1], Chenglong Li [1], Saqib Mujtaba [1], Xingming Ning [1,*], Pei Chen [1,*], Qiang Weng [1], Zhongwei An [1] and Xinbing Chen [1,*]

[1] Key Laboratory of Applied Surface and Colloid Chemistry (MOE), Ministry of Education, Shaanxi Key Laboratory for Advanced Energy Devices, Shaanxi Engineering Laboratory for Advanced Energy Technology, International Joint Research Center of Shaanxi Province for Photoelectric Materials Science, School of Materials Science and Engineering, Shaanxi Normal University, Xi'an 710119, China; xuli00@snnu.edu.cn (L.X.); jjquan2022@163.com (J.Q.); meihuali@snnu.edu.cn (M.L.); 330796680@snnu.edu.cn (C.L.); smujtaba304@gmail.com (S.M.); wengqiang@snnu.edu.cn (Q.W.); gmecazw@163.com (Z.A.)

[2] School of Chemistry and Chemical Engineering, Hexi University, Zhangye 734000, China; xuli_hxu@163.com

* Correspondence: ningxingming@snnu.edu.cn (X.N.); chenpei@snnu.edu.cn (P.C.); chenxinbing@snnu.edu.cn (X.C.)

† These authors contributed equally to this work.

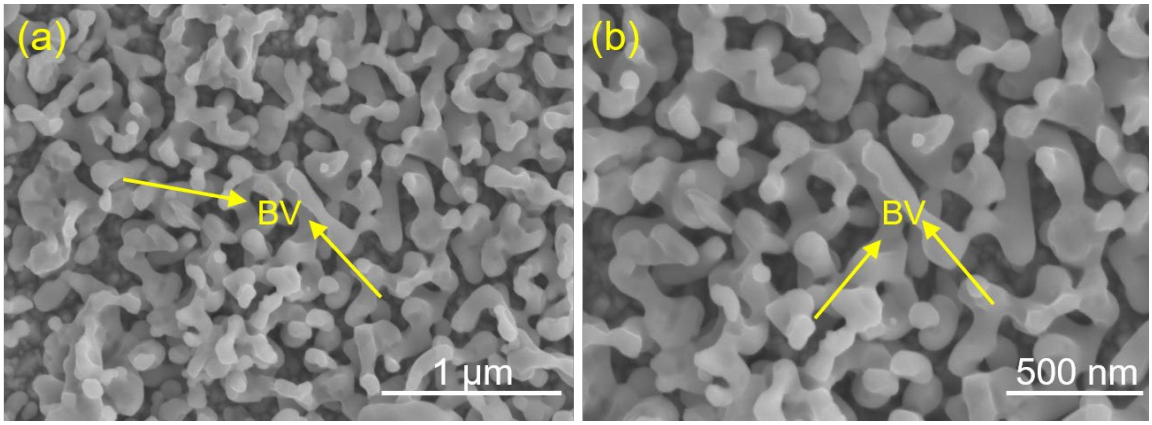

Figure S1. SEM images of the BV.

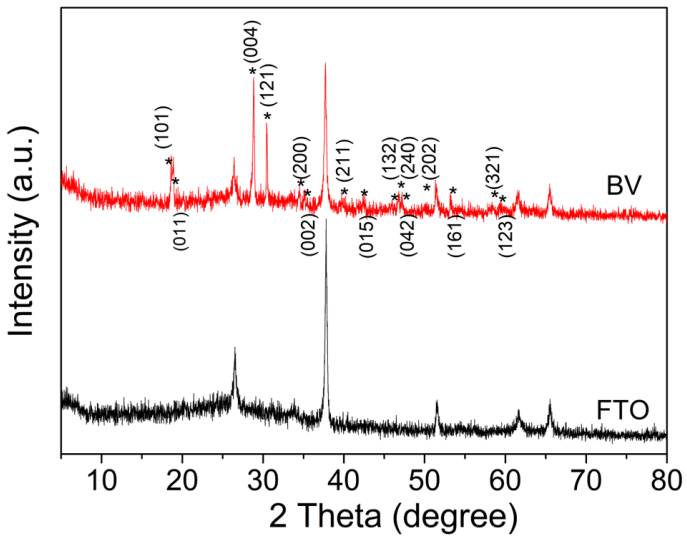

Figure S2. XRD of FTO and BV.

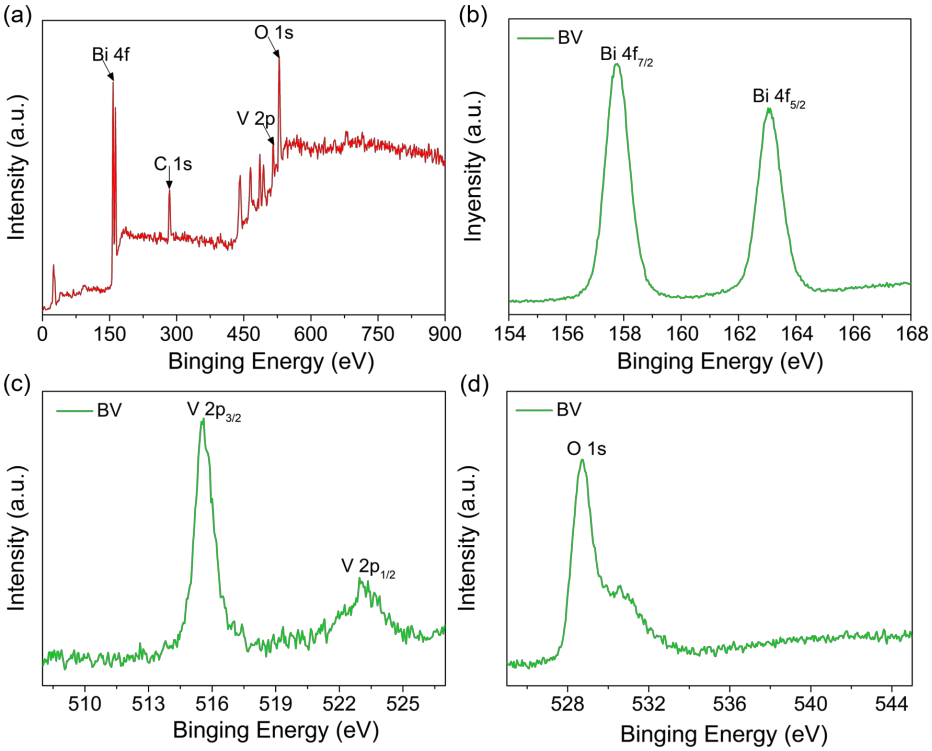

Figure S3. XPS spectra of BV.

As shown in Figure S3, the characteristic peaks of Bi 4f (b), V 2p (c), and O 1s (d) of BV can be detected from XPS results, meaning that the target has been successfully prepared, which are consistent with the previous reports[1-2].

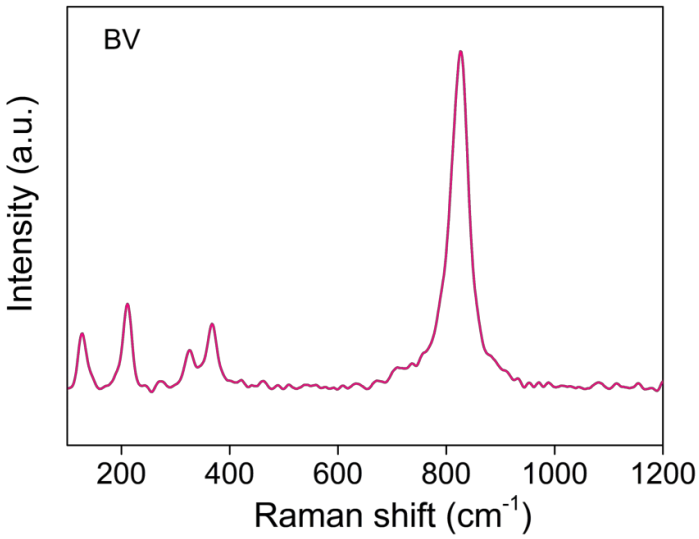

Figure S4. Raman spectra of BV.

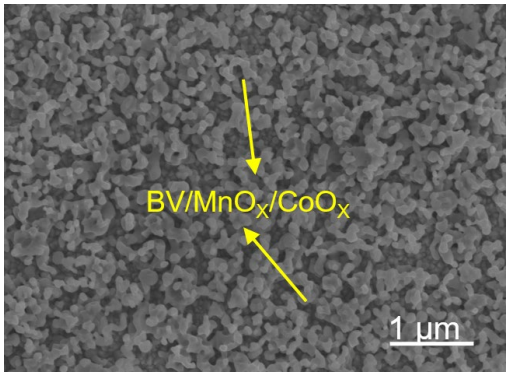

Figure S5. SEM image of BV/MnO_x/CoO_x.

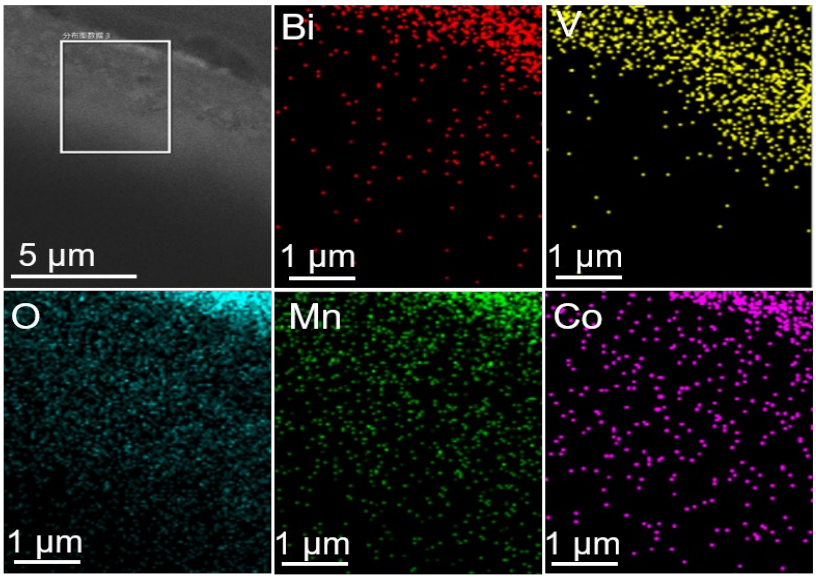

Figure S6. Cross-sectional SEM-Energy disperse spectroscopy (EDS) analysis of the BV/MnO_x/CoO_x.

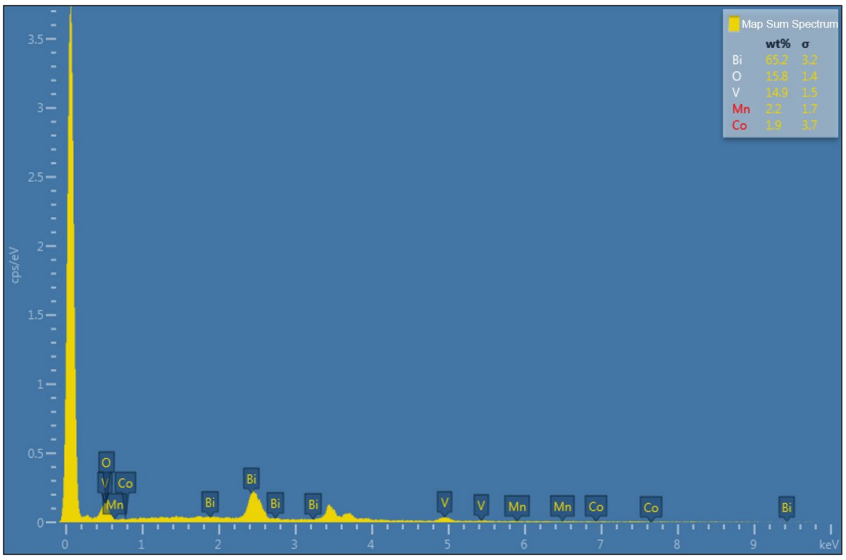

Figure S7. SEM-EDS spectra of BV/MnO_x/CoO_x.

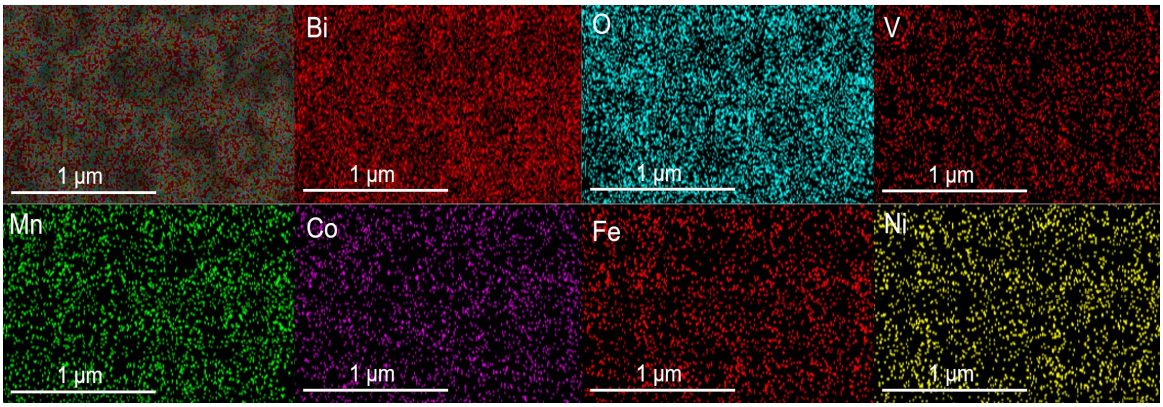

Figure S8. SEM-EDS elemental mapping images of BV/MnO_x/CoO_x/FeNiOOH.

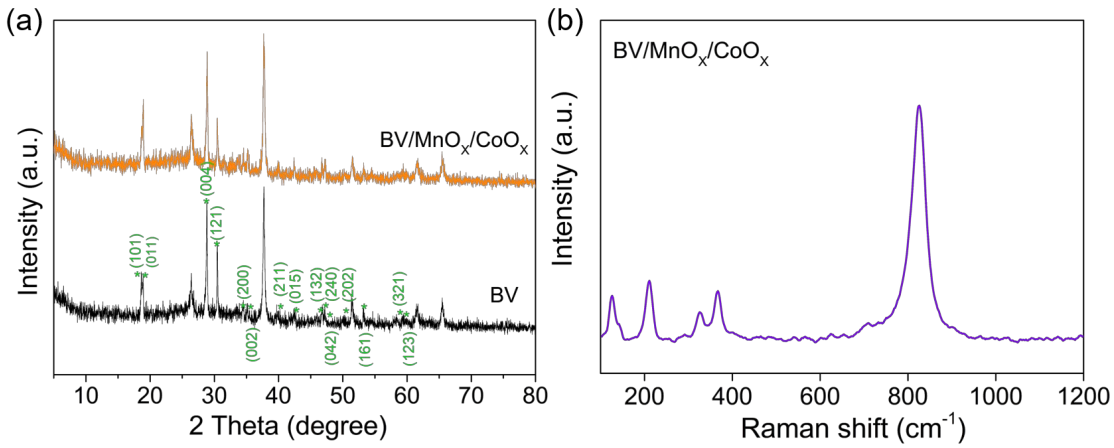

Figure S9. (a) XRD of BV and BV/MnO_x/CoO_x. (b) Raman spectra of BV/MnO_x/CoO_x.

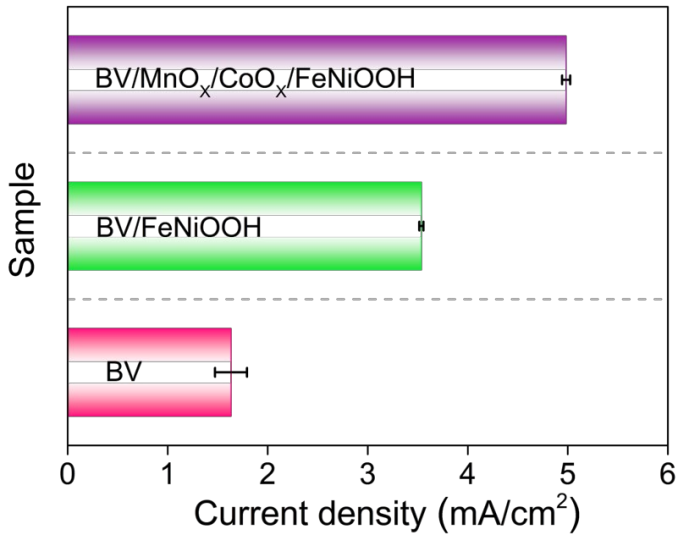

Figure S10. Photocurrent densities of BV/MnO_x/CoO_x/FeNiOOH, BV/FeNiOOH, and BV photoanodes.

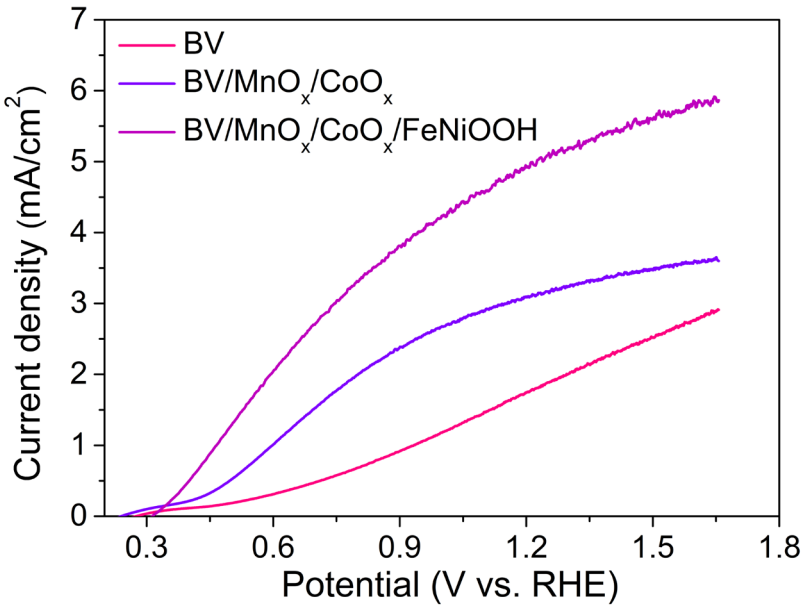

Figure S11. LSV curves of different photoanodes.

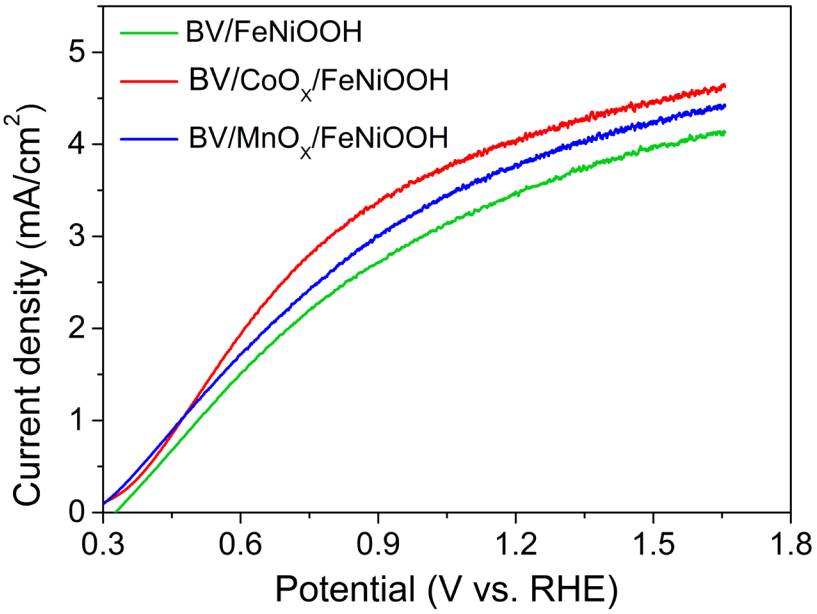

Figure S12. LSV curves of different photoanodes.

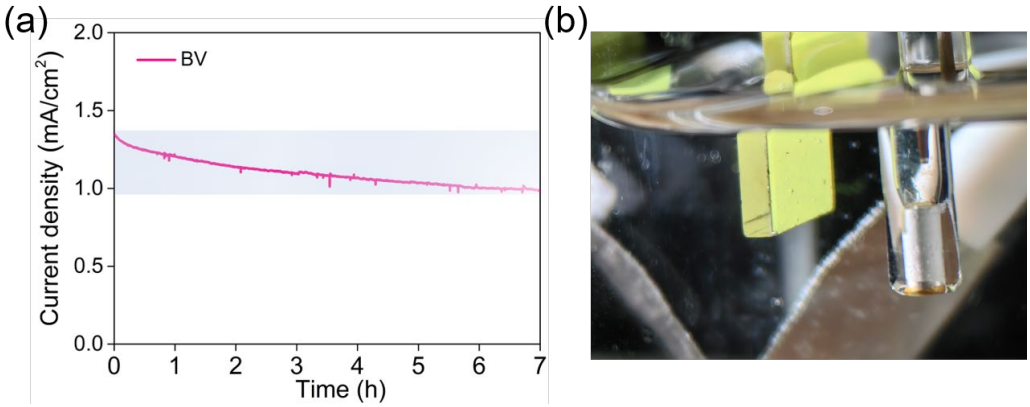

Figure S13. (a) *I-t* curve of the BV photoanode. (b) The picture of oxygen evolution.

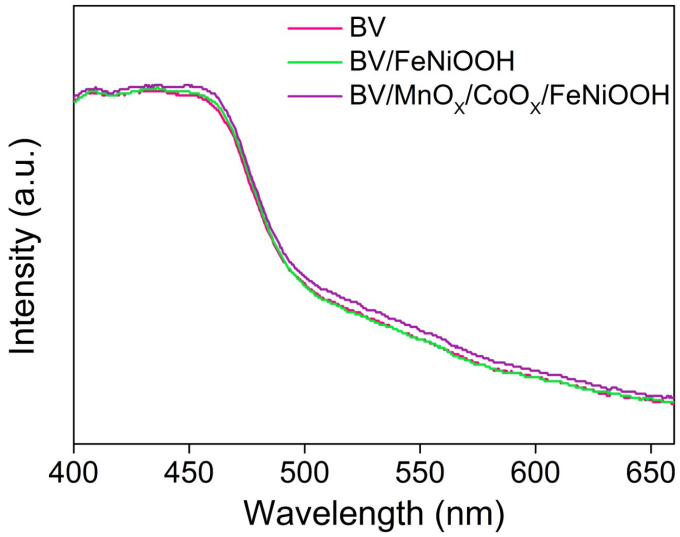

Figure S14. UV/Vis diffuse reflectance spectra of different samples.

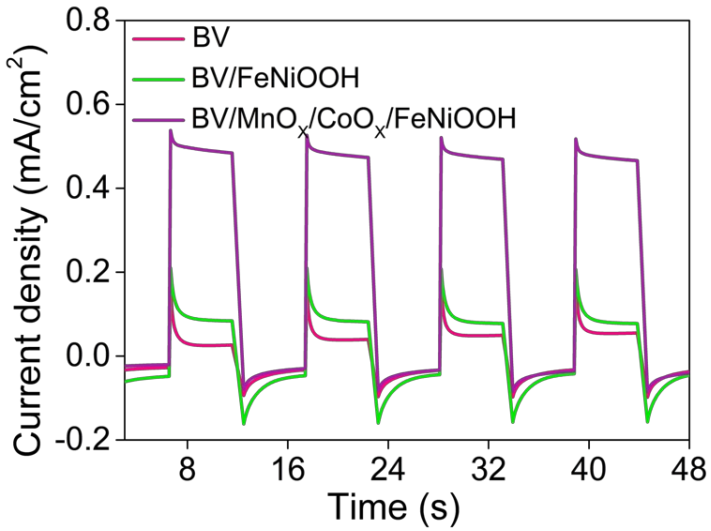

Figure S15. *I-t* curves of different photoanodes.

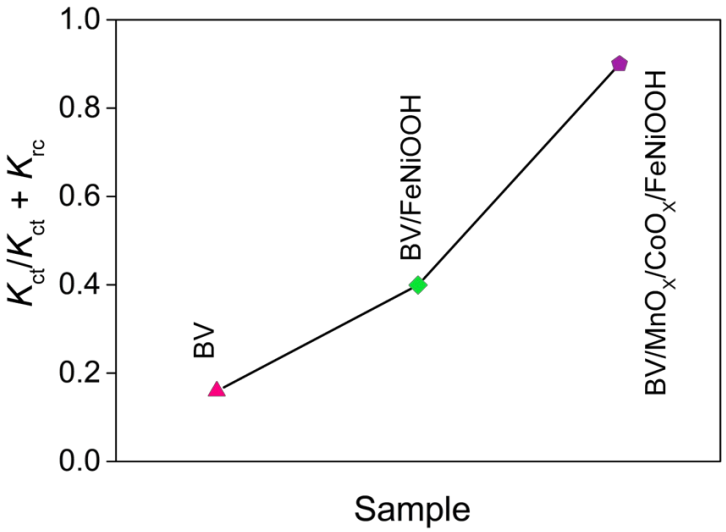

Figure S16. Charge transfer efficiencies for different samples.

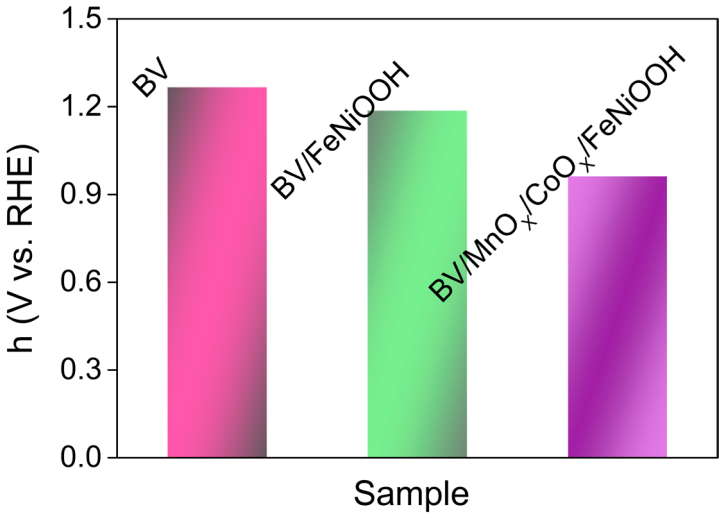

Figure S17. The overpotentials of different samples at 10 mA/cm^2.

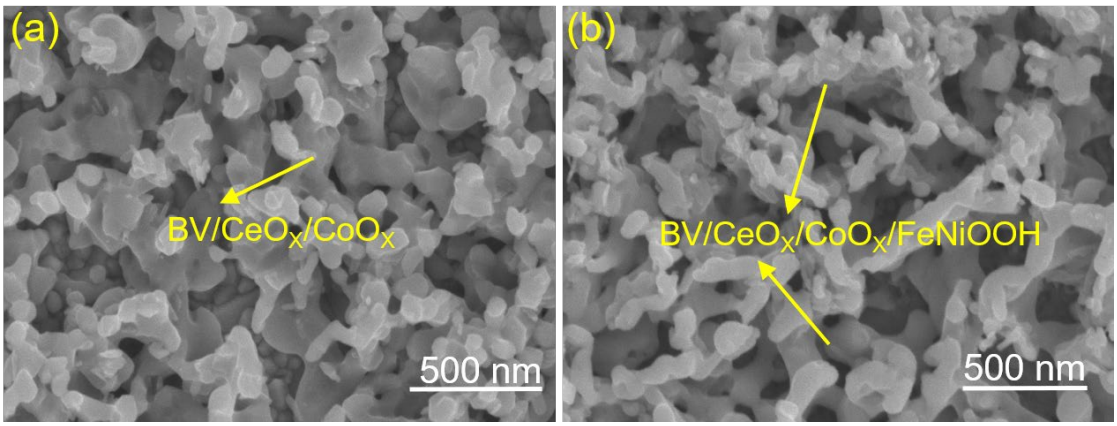

Figure S18. SEM image of (a) BV/CeO_x/CoO_x and (b) BV/CeO_x/CoO_x/FeNiOOH.

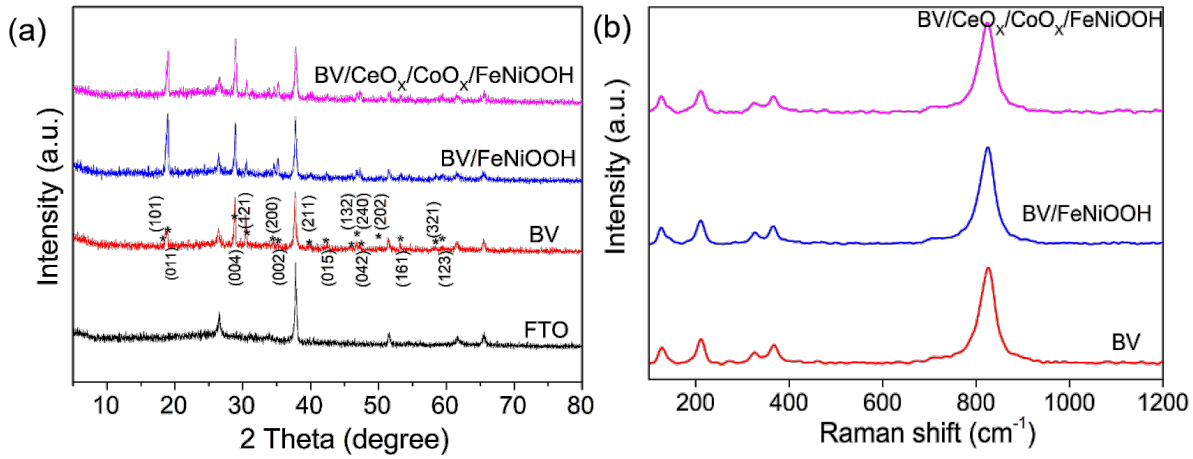

Figure S19. (a) XRD of FTO, BV, BV/FeNiOOH, and BV/CeO_x/CoO_x/FeNiOOH. (b) Raman spectra of different samples.

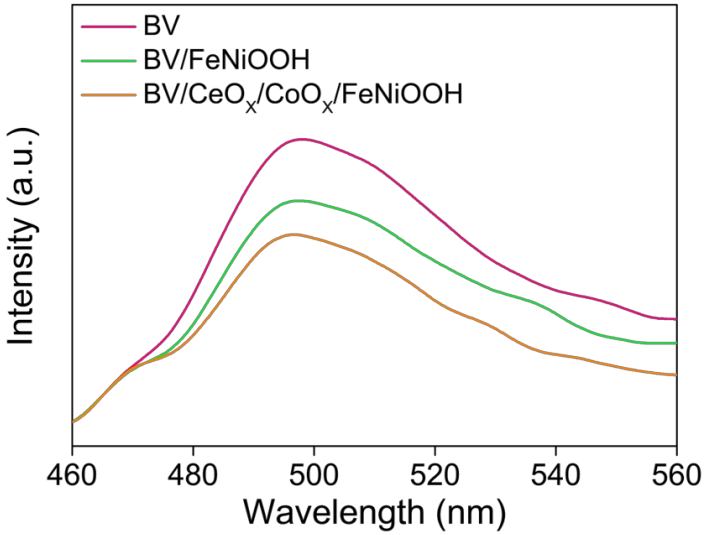

Figure S20. PL spectra of different photoanodes with excitation of 355 nm wavelength.

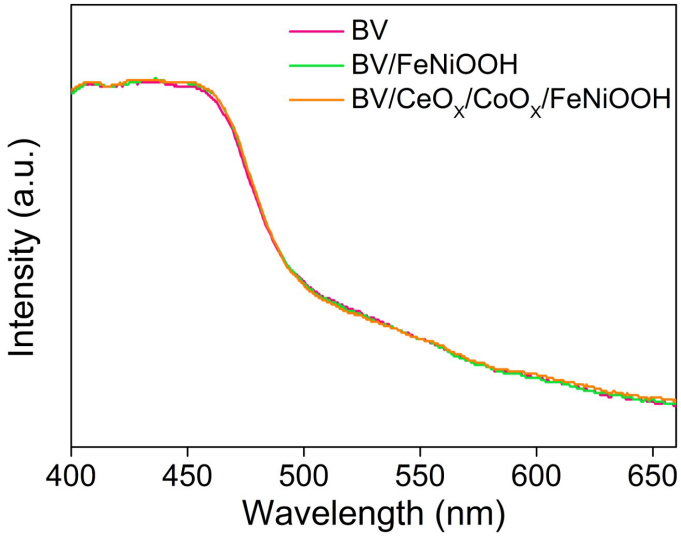

Figure S21. UV/Vis diffuse reflectance spectroscopy of different samples.

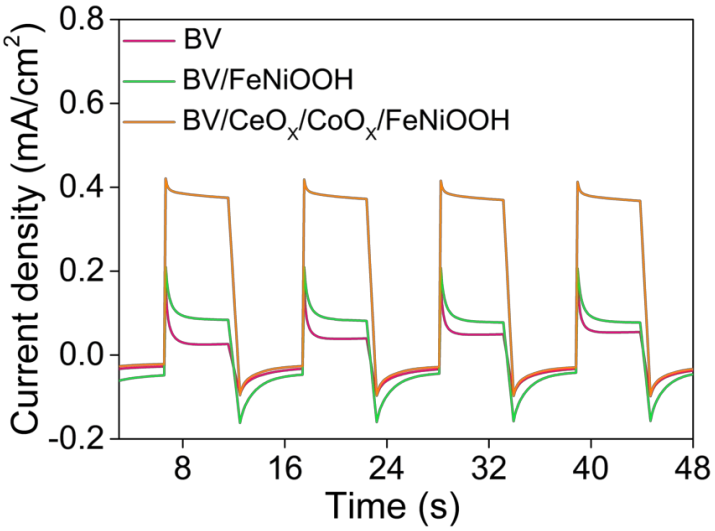

Figure S22. *I-t* curves of different photoanodes.

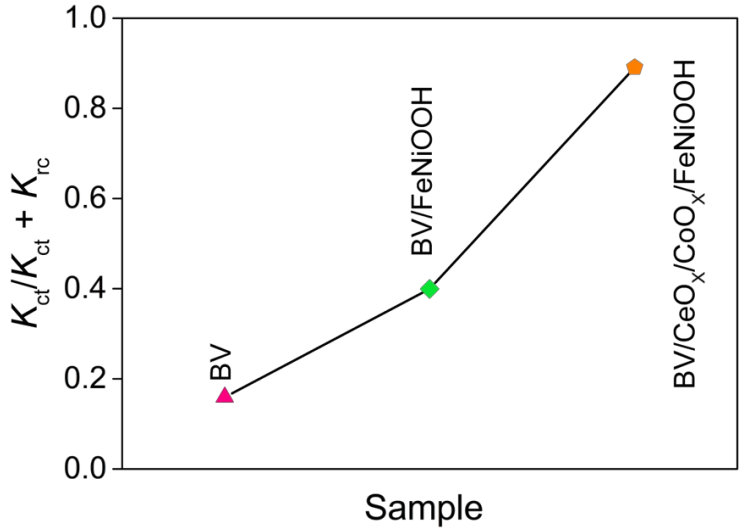

Figure S23. Charge transfer efficiencies.

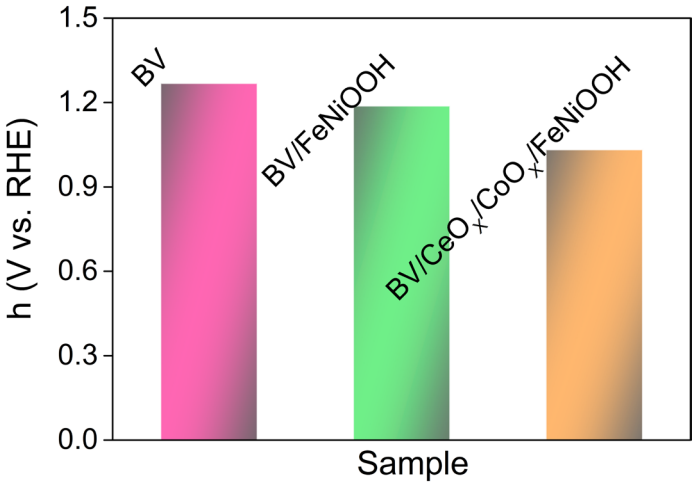

Figure S24. The overpotentials of different samples.

Table S1. EIS of different samples.

Samples	BV	BV/FeNiOOH	BV/MnO_x/CoO_x/FeNiOOH
R_s / (Ω)	41.9	44.4	43.4
R_{ct} / (Ω)	991	852	389

Table S2. Transit time values of different samples.

Samples	BV	BV/FeNiOOH	BV/MnO_x/CoO_x/FeNiOOH
f_{Imps} / (Hz)	121.15	316.23	464.16
τ_d / (ms)	1.31	0.50	0.34

Table S3. EIS of different samples.

Samples	BV	BV/FeNiOOH	BV/CeO_x/CoO_x/FeNiOOH
R_s / (Ω)	41.9	44.4	45.4
R_{ct} / (Ω)	991	852	522

Table S4. Transit time values of different samples.

Samples	BV	BV/FeNiOOH	BV/CeO_x/CoO_x/FeNiOOH
f_{Imps} / (Hz)	121.15	316.23	383.12
τ_d / (ms)	1.31	0.50	0.42

Reference

1. Zhang, X.; Zhai, P.; Zhang, Y.; Wu, Y.; Wang, C.; Ran, L.; Gao, J.; Li, Z.; Zhang, B.; Fan, Z.; Sun, L.; Hou, J. Engineering Single-Atomic Ni-N_4-O Sites on Semiconductor Photoanodes for High-Performance Photoelectrochemical Water Splitting. *Journal of the American Chemical Society* **2021,** *143* (49), 20657-20669.

2. Ning, X.; Du, P.; Han, Z.; Chen, J.; Lu, X. Insight into the Transition-Metal Hydroxide Cover Layer for Enhancing Photoelectrochemical Water Oxidation. *Angewandte Chemie International Edition* **2021,** *60* (7), 3504-3509.